

# Effects of noncovalently bound quinones on the ground and triplet states of zinc chlorins in solution and bound to *de novo* synthesized peptides†

Anke Mennenga, Wolfgang Gärtner, Wolfgang Lubitz and Helmut Görner\*

Received 21st August 2006, Accepted 12th October 2006

First published as an Advance Article on the web 30th October 2006

DOI: 10.1039/b612056c

The  $Q_y$  absorption band of two chlorophyll derivatives, zinc chlorin *e6* (ZnCe6) and zinc pheophorbide *a* (ZnPheida), in aqueous solution is bathochromically shifted on addition of quinones, e.g., 1,4-benzoquinone (BQ), with a corresponding shift of the fluorescence band. This is due to a complex formation of zinc chlorins induced by BQs and subsequent rearrangement. The time-resolved absorption spectra after laser pulse excitation show triplet quenching of the pigments by BQ and other quinones *via* electron transfer. The effects of electron transfer to noncovalently bound BQs were also studied with *de novo* synthesized peptides, into which ZnCe6 and ZnPheida were incorporated as model systems for the primary steps of photosynthetic reaction centers. Whereas the photophysical properties are similar to those of the unbound zinc chlorins, no BQ-mediated complex formation was observed.

## 1 Introduction

A major contribution to the remarkably high efficiency of photosynthesis is light-harvesting by the (bacterio)chlorophyll antenna system that transfers the light energy to the so-called reaction center before the electron is passed *via* chlorophyll derivatives to quinones. During these processes in the reaction center, chlorophylls serve as electron donors and as acceptors after electronic excitation. The initial photoproducts are radical ion pairs. Many of the primary processes in photosynthesis have been studied in great detail,<sup>1</sup> but still a number of open questions remain unsolved, in particular many aspects of the photophysical reactions of chlorophyll molecules. A major drawback for these studies is the strong electronic interaction of the many chlorophyll molecules in the antenna that makes it practically impossible to address a single entity in this large aggregated complex.

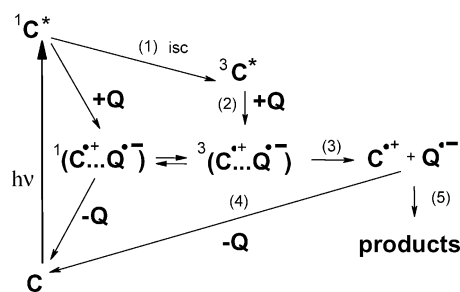
Since the photoprocesses of supramolecular aggregates involving chlorin moieties play a key role for photosynthesis in green plants and photosynthetic bacteria, many efforts have been made to describe the properties of chlorophyll assemblies.<sup>1–6</sup> The self-assembly of synthetic zinc chlorins in non-polar or aqueous microheterogeneous media to an artificial supramolecular light-harvesting device has been intensively investigated, see ref. 6 for a review. For chlorophyll *a* (Chl*a*)<sup>7–14</sup> and related pigments<sup>15–27</sup> many photophysical and photochemical properties have been reported. Furthermore, the intermediates in the photochemical reactions of Chl*a* are well characterized. It is known that the quantum yield of intersystem crossing ( $\Phi_{ISC}$ ) of aggregated Chl*a* is small, and monomeric Chl*a* in organic solvents shows both fluorescence and ISC in substantial quantum yields.<sup>11,12</sup>

Max-Planck-Institut für Bioanorganische Chemie, D-45413 Mülheim an der Ruhr, Germany. E-mail: goerner@mpi-muelheim.mpg.de; Fax: +49(0)2083063951; Tel: +49(0)2083063593

† Dedicated to Professor Kurt Schaffner on the occasion of his 75th birthday.

Chlorin *e6* (Ce6) remains monomeric when an organic solvent is replaced by water,<sup>20</sup> whereas pheophorbide *a* (Pheida) exists in a monomer–dimer equilibrium.<sup>23</sup> The low quantum yield of singlet molecular oxygen production ( $\Phi_{\Delta}$ ) for Pheida in aqueous solution, with respect to the value for the monomer in methanol, has been attributed to a low  $\Phi_{ISC}$  value due to the dimerization in water.<sup>16</sup> For a detailed analysis of the ground state interactions and electron transfer processes of the excited chlorins to noncovalently attached quinones, the zinc containing derivatives of Pheida and Ce6 were used in this work. Routinely, zinc complexes are preferentially used since no changes in the spectroscopic properties are to be expected by the exchange of magnesium into zinc; in addition, the zinc complexes show, amongst other experimental advantages, also a higher stability. The solubility of the pigments is of great importance when mimicking the primary photochemistry of pheophytin/quinone-type reaction centers. Therefore, the synthetic zinc chlorins in aqueous solution should include hydrophilic groups.<sup>6</sup>

Besides their photophysical behaviour, the interaction of chlorophylls with other molecules that serve as electron acceptors has been intensively studied. Scheme 1 shows the energy diagram of a chlorin (C) quinone (Q) pair. The excitation of an electron from the ground state of the chlorin as



Scheme 1

electron donor leads to the first excited state ( $^1C^*$ ), which is characterized by its electronic energy and by different vibrational states of the molecule. The excited chlorin can revert to the ground state in several ways, through internal conversion or fluorescence. Another pathway is ISC leading to the lowest triplet state ( $^3C^*$ ). The quinone as electron acceptor quenches the  $^1C^*$  or  $^3C^*$  states by formation of the correlated radical pairs:  $^1(C^{\bullet+}..Q^{\bullet-})$  and  $^3(C^{\bullet+}..Q^{\bullet-})$ , where the former is only involved at high BQ concentrations. A direct electron transfer from the  $^3C^*$  state to a quinone can be observed by transient absorption spectroscopy, whereby the rate constant for the triplet decay and the appearance of the radical cation  $C^{\bullet+}$  should be the same. In particular the Chla/BQ system was studied in non-aqueous solution by flash photolysis and electron spin resonance spectroscopy.<sup>7-12</sup>

Photoprocesses of other tetrapyrroles and related chromophores with quinones in solution have been examined in great detail.<sup>28-33</sup> These investigations have revealed a broad variation of interactions and reactivities: preferentially the system of zinc *meso*-tetrakis(sulfonatophenyl)porphyrin and 2,3-dimethoxy-5-methyl-1,4-benzoquinone (UQ<sub>0</sub>) undergoes electron transfer in the triplet state and the excited singlet state.<sup>29</sup> Both the excited singlet and triplet states are also quenched by BQ for tetraphenylporphyrin in dichloromethane.<sup>30</sup> In contrast, any detailed knowledge concerning photoinduced intermolecular electron transfer from chlorins in aqueous solution is still scarce.

A useful approach is the investigation of simple model systems with the aim of obtaining information about general mechanisms leading to radical pairs. Incorporation of metallochlorins into *de novo* synthesized proteins provides the possibility to study the photochemical reaction of monomeric chlorins, and upon addition of an electron acceptor, to mimic electron transfer proteins found in photosynthesis and respiration.

Much effort has been made to mimic the function of reaction centers in peptide models.<sup>34-39</sup> Related to the present work, *de novo* designed four-helix bundle proteins with metalloporphyrin cofactors were characterized and anthraquinone-2-sulfonate was used for photoinduced electron transfer from peptide-bound zinc protoporphyrin IX.<sup>35a</sup> Photoinduced electron transfer from ZnCe6 in aqueous solution to free phenyl-*p*-benzoquinone (phBQ) and covalently bound UQ<sub>0</sub> was observed by EPR.<sup>37,38</sup> The reaction from excited ZnCe6 to phBQ was reported to be faster and to have a higher yield in the presence of a peptide maquette.<sup>36</sup> When UQ<sub>0</sub> is covalently attached *via* a cysteine to a protein as ZnCe6-cytochrome *b*<sub>562</sub>, electron transfer takes place. Static quenching was also suggested based on the shorter fluorescence lifetime ( $\tau_f$ ).<sup>37</sup> This raises the question of the specific features of synthetic proteins and their contributions to the reactivity of the incorporated cofactors.

In this study, we investigated the ground state interactions of ZnCe6 and ZnPheida and some related pigments with

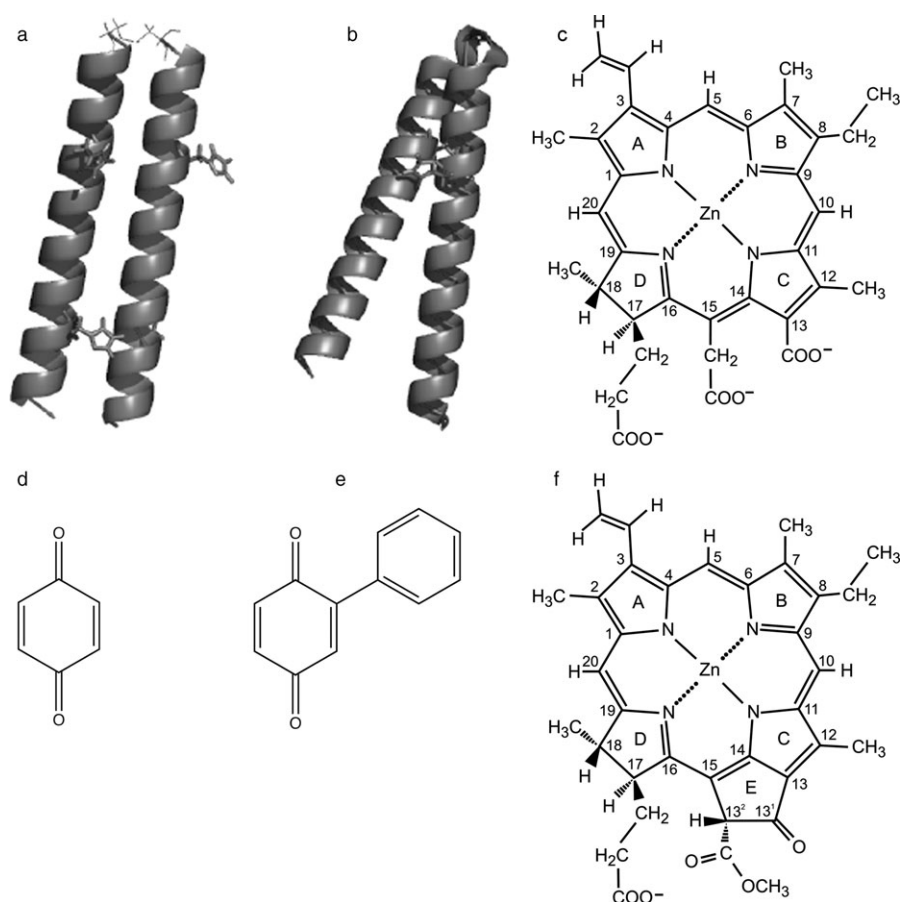


**Fig. 1** Schematic representation of the structures of the peptides (a) M1, (b) M2 and (c) ZnCe6, (d) BQ, (e) phBQ and (f) ZnPheida.

quinones in solution (see Fig. 1) and after binding to two peptide maquettes (M1 and M2) as well as their triplet state reactions. There are two major questions to be asked: do synthetic proteins affect the electron transfer from the zinc chlorin excited states to BQs? What is the nature of the complex formed between zinc chlorin and BQ in aqueous solution? We have addressed these questions by measuring spectral and kinetic data, using BQ, phBQ and methyl viologen ( $MV^{2+}$ ) as electron acceptors. We show that the quenching rate constant of zinc chlorins by BQs depends on several factors, albeit the mechanism is the same either in solution or bound into the four-helix bundle.

## 2 Experimental

The compounds phBQ (Acros),  $MV^{2+}$  (Aldrich), *Ce6* (Frontier Scientific) and the solvents (Merck) were used as commercially received or purified by sublimation (BQ) or distillation (methanol). Water from a Millipore apparatus was applied throughout. All measurements were performed under dimmed light conditions at room temperature unless otherwise indicated.

### 2.1 Pigment preparation

*Chla* was isolated from *Spirulina platensis* by methanol extraction and purified by reverse phase high performance liquid chromatography (RP-HPLC) using a Nucleosil-5-C18 column (Macherey & Nagel),  $125 \times 8$  mm. Methanol was used as elution solvent (flow rate  $1.5 \text{ ml min}^{-1}$ ). Pheida was prepared by treatment of  $0.14 \text{ mol Chla}$  with pure trifluoroacetic acid for 30 min. After evaporation of the acid, Pheida was purified by RP-HPLC (methanol, flow rate:  $1.5 \text{ ml min}^{-1}$ ).

ZnPheida was synthesized from Pheida by dissolving the latter in pure acetic acid and addition of a 250-fold molar excess of zinc acetate, 20-fold molar excess of sodium acetate, and catalytic amounts (10–50 mg) of sodium ascorbate. This reaction mixture was stirred for 1 h. The product was purified by RP-HPLC, Nucleosil-5-C18, methanol/0.5 M ammonium acetate (8 : 1, v/v), flow rate  $1.5 \text{ ml min}^{-1}$ , followed by desalination with diethyl ether and water. The solution was dried over sodium sulfate and the organic phase removed by evaporation. Since the pigment is insoluble in water, it was dissolved in acetone prior to preparation of aqueous solutions for the spectroscopic measurements. The amount of acetone in each experiment did not exceed 6%.

Zn*Ce6* was synthesized from *Ce6* by addition of molar equivalents of zinc acetate to a buffered aqueous solution (25 mM glycine, 50 mM NaCl, pH 10) and stirring for 30 min at  $4 \text{ }^\circ\text{C}$  in argon atmosphere. The reaction was monitored by UV-Vis spectroscopy, probing a red shift of the Soret band ( $401 \rightarrow 412 \text{ nm}$ ) and a blue shift of the  $Q_y$  band ( $655 \rightarrow 633 \text{ nm}$ ). In addition, Zn*Ce6* was separated from metal free *Ce6* by RP-HPLC, Kromasil-5-C18 (MZ-Analytentechnik),  $125 \times 4.6$  mm, 50 mM triethylammonium acetate (pH 8)/methanol (1 : 2, v/v, flow rate  $0.8 \text{ ml min}^{-1}$ ) with a purity of 94.5%. The pigments were stored under argon at  $-80 \text{ }^\circ\text{C}$  until use. All preparations were performed under green light.

### 2.2 Peptide synthesis

Maquette M1: The concept for this peptide is based on a prototype peptide design known as “H10H24” which is modelled from known sequences of the cytochrome *bc*<sub>1</sub> respiratory complexes. It was originally synthesized to investigate heme binding peptides.<sup>38</sup> The sequence of the  $\alpha$ -helical peptide is identical to that used by Fahnenschmidt *et al.*:<sup>35b</sup> C-G-G-G-E-L-W-K-L-H-E-E-L-L-K-K-F-E-E-L-L-K-L-H-E-E-R-K-K-K-L. The  $\alpha$ -helical peptide was synthesized as a 31-amino acid stretch that was subsequently homodimerized through the N-terminal cysteine in 0.05 M ammonium acetate at pH 7.6 with 2% DMSO to form a disulfide linked 62-mer peptide.

Maquette M2: Design of this peptide is based on the work of Sharp *et al.*<sup>39</sup> with the following sequence: L-K-K-L-R-E-E-A-L-K-L-L-E-E-F-K-K-L-L-E-E-H-L-K-W-L-E-G-G-G-G-G-G-G-E-L-L-K-L-H-E-E-L-L-K-K-C-E-E-L-L-K-L-A-E-E-R-L-K-K-L. The histidine as the axial ligand for the cofactor is located in the centre of the hydrophobic core inside the formed four-helix bundle maquettes. The ligand position was also verified by 2D-Pulse-ESEEM spectroscopy.<sup>40</sup>

The peptides M1 and M2 were synthesized on an automated peptide synthesizer (Advanced ChemTech, 348 $\Omega$ ) using Fmoc-protected amino acids (Novabiochem and Iris Biotech) on a PAL-PEG-PS resin (Applied Biosystems). N-terminal acetylation of the peptides was performed with 5% acetic anhydride in dimethylformamide prior to cleavage. Purification of the crude peptides was performed by RP-HPLC (Vydac Protein & Peptide), C18 column,  $250 \times 22$  mm, aqueous/acetonitrile gradients containing 0.1% trifluoroacetic acid, flow rate  $10 \text{ ml min}^{-1}$ . The molecular mass of the purified peptides was verified by MALDI-TOF-MS, M1: calcd 7607 Da, found 7609 Da; M2: calcd 7179 Da, found 7181 Da. A yield of 8% of the maquette M2 was determined.

### 2.3 Metallochlorin incorporation into peptides

The synthetic metallopeptides were prepared by slow addition of an excess of the metallochlorin solution, Zn*Ce6* in glycine buffer, ZnPheida dissolved in acetone, to the peptide with gentle stirring for 30 min at  $4 \text{ }^\circ\text{C}$  in the dark. The pigment-peptide complex was separated from unbound pigment by using a Pharmacia PD-10 column, which was equilibrated with 50 mM potassium phosphate buffer (100 mM KCl) at pH 7.3.

### 2.4 Solution molecular weight determination

A FPLC system (ÄKTA basic) equipped with a Superdex 75 HR10/30 column (all Amersham Biosciences) equilibrated at a flow rate of  $0.5 \text{ ml min}^{-1}$  with 150 mM NaCl and 50 mM phosphate buffer (pH 7.3) was used for gel-filtration chromatography with detection wavelengths of 260 and 280 nm. Column calibration was performed with a low molecular weight gel filtration calibration kit (Amersham Biosciences) and aprotinin (Roth). The different zinc chlorin peptide scaffolds elute with retention times consistent with a dimer of the complex, *i.e.*, four-helix bundles, with less than 8% of the material comprising higher oligomerization states.

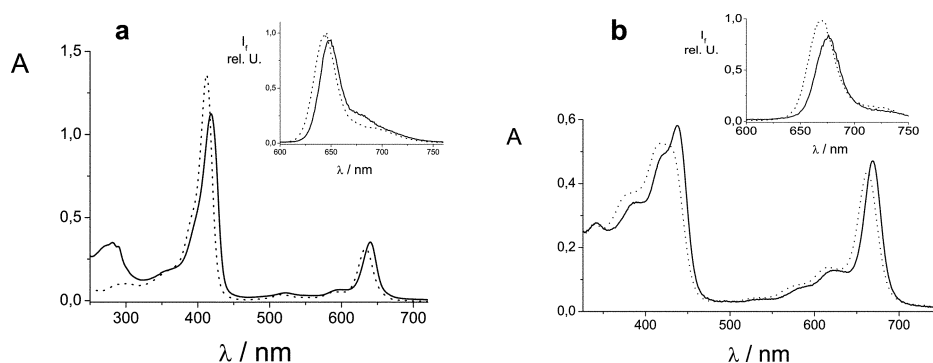


**Fig. 2** Absorption and fluorescence spectra (insets) of (a) 8  $\mu\text{M}$  ZnCe6 and (b) 9  $\mu\text{M}$  ZnPheida in 0.05 M phosphate buffer at 24  $^{\circ}\text{C}$ , pH 7.3, (dotted line) and incorporated in the peptide M2 (solid line).

## 2.5 UV-Vis spectroscopy

The steady-state absorption spectra were recorded in 1 cm cuvettes on spectrophotometers (either Varian Cary 5 or HP 8453). The molar absorption coefficients in aqueous solution are  $\epsilon_{667} = 4.5 \times 10^4 \text{ M}^{-1} \text{ cm}^{-1}$  for Pheida,<sup>23</sup>  $\epsilon_{663} = 4.7 \times 10^4 \text{ M}^{-1} \text{ cm}^{-1}$  for ZnPheida and  $\epsilon_{633} = 4.0 \times 10^4 \text{ M}^{-1} \text{ cm}^{-1}$  for ZnCe6. The pigment concentrations were 5–10  $\mu\text{M}$  in 0.01–50 mM phosphate buffer (100 mM KCl, pH 7.3) or in 25 mM glycine buffer (50 mM NaCl, pH 10).

## 2.6 Fluorescence spectroscopy

The fluorescence spectra were recorded on a Varian Cary-Eclipse spectrofluorimeter. The quantum yields of fluorescence were obtained from the emission areas with optically matched solutions ( $\lambda_{\text{exc}} = 418 \text{ nm}$ ) using Chla in acetone with  $\Phi_f = 0.24$  as reference.<sup>7</sup> The fluorescence decay kinetics were determined by a fluorimeter (Edinburgh Instr. F900) with a time resolution of 0.2 ns,  $\lambda_{\text{exc}} = 385 \text{ nm}$ . The experimental error of  $\tau_f$  is  $\pm 0.2 \text{ ns}$ , that of  $\Phi_f$  is  $\pm 10\%$  for values larger than 0.1 and  $\pm 20\%$  otherwise. The absorption and fluorescence measurements refer to air-saturated solutions unless otherwise indicated.

## 2.7 Transient absorption spectroscopy

The time-resolved measurements were carried out with a tunable laser (Opotek, Vibrant 355II) pumped from a Nd-YAG and using an OPO, pulse width: 5 ns, energy per pulse:

up to 10 mJ,  $\lambda_{\text{exc}} = 410\text{--}710 \text{ nm}$ . The set-up contains a 150-W Xenon lamp and a home-made pulser, a monochromator with stepper motor, a photomultiplier (Hamamatsu R955) and two transient digitizers (Tektronix, 7912AD and 390AD). Chla in ethanol was used as reference with  $\Phi_{\text{ISC}} = 0.5$ .<sup>17</sup> The experimental error of  $\tau_T$ ,  $k_{\text{ox}}$ ,  $k_q$  is  $\pm 10\%$ , that of  $\Phi_{\text{ISC}}$  is  $\pm 15\%$  for values larger than 0.2 and  $\pm 30\%$  otherwise. The solutions were freshly prepared and immediately photolyzed, especially at pH 10 and for zinc chlorin/quinone systems at pH 7.3. When complex formation is involved, the T–T absorption at 450–600 nm is lower and the bleaching is broader. The low temperature measurements were carried out in aqueous buffer and glycerol (2 : 3, v/v) using cooled nitrogen.

## 3 Results

### 3.1 Steady state absorption

The incorporation of the zinc chlorins into the four-helix bundles and the steady state interaction of zinc chlorins (in solution and in peptide-bound form) with quinones was investigated by UV-VIS absorption spectroscopy. The maxima of the ground state absorption spectrum of ZnCe6 in aqueous solution in the presence of phosphate buffer (pH 7.3) are at 412 and at 633 nm (Soret and  $Q_y$  band, respectively). The bands are red-shifted to 421 and 642 nm for ZnCe6 incorporated in maquette M1 and 419 and 640 nm for ZnCe6 bound to maquette M2 (Fig. 2a). Analogous shifts were found

**Table 1** Absorption and fluorescence properties of chlorins<sup>a</sup>

Compound	Quinone <sup>b</sup>	$\lambda/\text{nm}$	$\lambda_f^c/\text{nm}$	$\Phi_f$	$\tau_f^d/\text{ns}$
Ce6	None or BQ	401, 655	662		
ZnCe6	None	412, 633	643	0.32	2.1
	BQ	412, 673	684		
	phBQ	412, 673	684		
ZnCe6-M1	None or BQ	421, 642	647	0.29	2.2
ZnCe6-M2	None or BQ	419, 640	647	0.29	2.2
ZnPheida	None	425 <sup>e</sup> , 663	669	0.03	3.4
	BQ	425 <sup>e</sup> , 740			
	phBQ	425 <sup>e</sup> , 738			
ZnPheida-M1	None or BQ	437, 669	674	0.02	3.1
ZnPheida-M2	None or BQ	433, 668	677	0.02	3.1

<sup>a</sup> In air-saturated aqueous solution at 24  $^{\circ}\text{C}$  and 0.01 M phosphate buffer, pH 7.3. <sup>b</sup> Typical concentration 10–200  $\mu\text{M}$ . <sup>c</sup>  $\lambda_{\text{exc}} = 420 \text{ nm}$ . <sup>d</sup> Values refer to the main component (70–90%); same values in argon-saturated solution. <sup>e</sup> Broad signal due to aggregation.

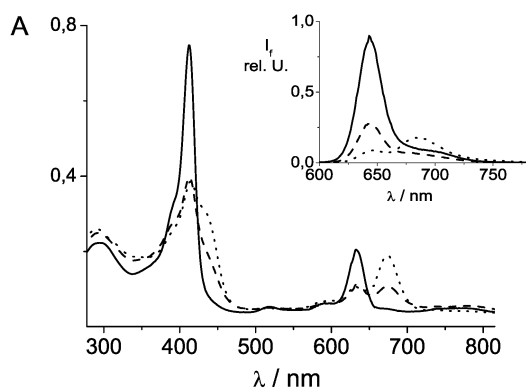


**Fig. 3** Absorption spectra of 4  $\mu\text{M}$  ZnCe6 in 0.01 M phosphate buffer at 24  $^{\circ}\text{C}$ , pH 7.3, directly upon addition of 20  $\mu\text{M}$  BQ (solid line) and after 200 and 600 s (dashed and dotted line); inset: corresponding fluorescence spectra ( $\lambda_{\text{exc}} = 418$  nm) prior to mixing with 20  $\mu\text{M}$  BQ and after 150 and 1000 s (solid, dashed and dotted lines), respectively.

for ZnPheida in solution and ZnPheida bound to the peptides M1 and M2 (Fig. 2b and Table 1), *e.g.*, 663 to 669/668 nm, respectively. These effects were taken as evidence for the ligation of the pigment to the peptide (also according to literature data),<sup>34–39</sup> which is assumed to form a four-helix bundle as indicated by gel-filtration.

Addition of a five-fold excess of BQ and stirring for a short-time leads to a decrease of the absorption of the  $\text{Q}_y$  band of ZnCe6 and creates an additional band at 673 nm with “quasi”-isobestic points at 422 and 646 nm (Fig. 3). The steady state spectrum is fully developed within 1 h. The decrease of the  $\text{Q}_y$  band absorption is faster when the BQ concentration is increased, see kinetics in Fig. 4a and b for a five- and a forty-fold excess of BQ, respectively. The five-fold excess of BQ leads to a rate constant of decay ( $k_-$ ) of  $k_- = 0.008 \text{ s}^{-1}$  and to a rate constant of grow-in ( $k_+$ ) of  $k_+ = 0.0001 \text{ s}^{-1}$  of the absorption bands, whereas a forty-fold excess of BQ gave  $k_- = 0.03 \text{ s}^{-1}$  and  $k_+ = 0.002 \text{ s}^{-1}$ . A potential influence of the buffer components (suggested salt effect) was tested by repeating the experiment in distilled water, which gave rise to the same spectral features, although the reaction rate is larger under buffered conditions. Each of the parameters pH (between 6 and 8), concentration of zinc chlorin and buffer influences the reaction. The contribution of these parameters to the kinetics was not separated. The only significant effect

comes from the BQ concentration on the kinetics of the first step (Fig. 4).

Most interestingly, virtually no spectral changes were registered for the metal-free chlorins, Ce6 and Pheida, under the same experimental conditions. The course of the reaction changes drastically at alkaline pH ( $\sim 10$ ). Under these conditions, applied also by Razeghifard and Wydrzynski<sup>36</sup> on the same system, a competing side reaction interferes with the previously described quinone-mediated complex formation: the added quinone rapidly converts into the hydroquinone—this process being observable spectroscopically—and prevents complex formation. This thermal reaction can be stopped when air is removed, and the complex with identical spectral properties as described above was observed, indicating that the chlorin/BQ solution requires a less alkaline environment or the absence of oxygen.

For ZnPheida in phosphate buffer at pH 7.3 a two-step pattern was also found and an even larger shift from 663 to 740 nm upon addition of a forty-fold excess of BQ (not shown) with a decrease of the  $\text{Q}_y$  band at 663 nm. For BQ and both zinc chlorins the total  $\text{Q}_y$  absorbance decreases initially and reappears at a later time and at a longer wavelength. The pronounced bathochromic shifts are reminiscent to coordination of the metal by water.<sup>13</sup>

In order to investigate whether a strong ligation to the zinc chlorins affects the shifts of the absorption bands, imidazole as a commonly used ligand for porphyrins<sup>41</sup> was applied. Upon addition of imidazole to ZnPheida, a new absorption band at 685 nm due to ligation of the imidazole to the ZnPheida is detectable, whereas the band at 663 nm decreases (not shown). The smaller shift with respect to those of quinones indicates a different type of interaction. Finally, it should be pointed out that the shifts observed upon addition of a quinone are in contrast to the results found for the four synthetic metallopeptides (ZnCe6-M1, ZnCe6-M2, ZnPheida-M1, ZnPheida-M2), for which no spectral changes on addition of BQ were observed under the same experimental conditions (Table 1).

### 3.2 Fluorescence spectroscopy

Fluorescence as well as steady-state absorption spectroscopy, yields valuable information on the ligation of the zinc chlorins into the four-helix bundle peptides and the interaction of the quinone to the pigments. The fluorescence spectra of ZnCe6 and of ZnPheida in aqueous solution in the presence of

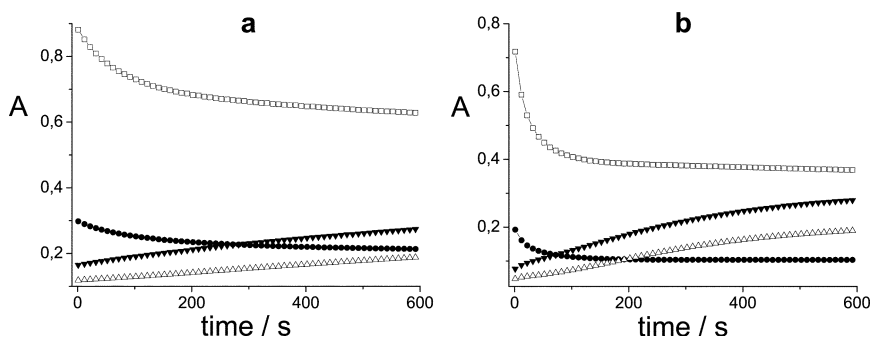


**Fig. 4** Kinetic traces of 4  $\mu\text{M}$  ZnCe6 in 0.01 M phosphate buffer at 24  $^{\circ}\text{C}$ , pH 7.3, upon addition of a (a) low BQ- (20  $\mu\text{M}$ ) and (b) high BQ-concentration (170  $\mu\text{M}$ ) at characteristic wavelengths of 410 ( $\square$ ), 630 ( $\bullet$ ), 675 ( $\Delta$ ) and 440 ( $\blacktriangledown$ ) nm.

0.1–10 mM phosphate buffer at pH 7.3 have emission maxima at  $\lambda_f = 643$  and 669 nm, respectively (Fig. 2a and b, insets). The fluorescence excitation spectra are in accord with the absorption data. The synthetic metallopeptides show emission maxima at  $\lambda_f = 647$  nm for ZnCe6, bound to maquette M1 as well as to maquette M2 and 674/677 nm for ZnPheida-M1/-M2 systems, respectively. These bathochromic shifts of the fluorescence bands confirm the ligation of the pigments into the *de novo* synthesized peptides.

The fluorescence quantum yield is  $\Phi_f = 0.29$ –0.32 for ZnCe6 in the absence or presence of M1/M2 and is much smaller for ZnPheida and the ZnPheida-M1/-M2 systems. This result provides evidence of the presence of monomeric ZnCe6, whereas ZnPheida aggregates in aqueous solution. The major fluorescence decay component corresponds to  $\tau_f = 2$ –3 ns (Table 1). Virtually no change in  $\tau_f$  was observed in the absence or presence of air as well as upon addition of *ca.* 0.05 mM BQ, indicating no fluorescence quenching by the quinone.

In accordance with the results of the absorption spectroscopy, the intensity of the emission maximum of ZnCe6 decreases in the presence of BQ and a new band at 684 nm appears (Fig. 3). The BQ-induced steady state spectrum is not specific for BQ, as we also found similar effects with pHBQ. The fluorescence emission spectra of either the metal-free chlorins or the synthetic metallopeptides are essentially unchanged upon addition of BQ, this is similar to the results from absorption spectroscopy. It is noteworthy that the ground state absorption and fluorescence spectra of chlorophylls are as yet not known to be affected by BQs.

### 3.3 Triplet state

In addition to steady state measurements, transient absorption spectroscopy was performed. It provides the possibility to investigate the excited states of the pigments in a time-resolved manner. The triplet state of the pigments can be characterized and quenching processes with quinones, indicating electron transfer and formation of radical pairs, can be investigated. The results refer to 0–2 min. after mixing, *i.e.*, under conditions where the complex between a zinc chlorin and BQ is formed to less than 10%. The transient spectrum of ZnCe6 in phosphate buffer shows two bleaching signals at 400 and 635 nm which refer to the bleached ground state absorption bands and transient absorption everywhere else (Fig. 5a). The spectra of ZnPheida (Fig. 6a), the peptide-bound pigments (Fig. 7a and 8a), and Ce6 show identical features upon excitation except for the bleaching bands which are in accordance with their absorption maxima. The transient species appears within the duration of the laser pulse and decays by first-order kinetics under argon and at low laser intensities. The lifetime ( $\tau_T$ ) decreases in air and yields a rate constant for quenching by oxygen of  $k_{ox} = (0.1$ –1.5)  $\times 10^9$   $M^{-1} s^{-1}$  (Table 2). In water,  $k_{ox}$  is lower and  $\tau_T$  is longer than in a water-free environment. The transient species that is formed during the pulse is assigned to the lowest triplet state of the chlorin. This behaviour is similar to that of the monomeric triplet state of Chla in, *e.g.*, acetone or ethanol, where the bleaching maxima are at 420 and 635 nm and  $\tau_T = 30 \pm 3$   $\mu s$  (acetone) and  $90 \pm$

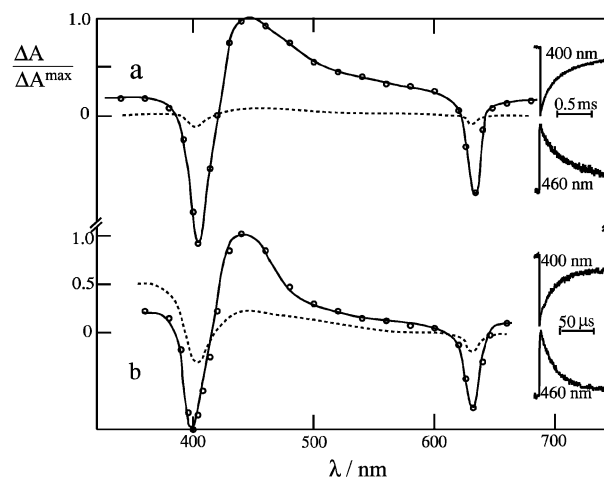


**Fig. 5** Transient absorption spectra of 5  $\mu M$  ZnCe6 in argon-saturated 0.01 M phosphate buffer at 24  $^{\circ}C$ , pH 7.3, (a), (b) solid line: at the end of the 420 nm pulse; (a) no additive (broken line: after 1 ms) and (b) in the presence of BQ (10  $\mu M$ , broken line: after 0.1 ms); insets: kinetic traces for 400 and 460 nm as indicated. Note that the results refer to conditions, where the proposed complex was not formed in measurable yield.

10  $\mu s$  (ethanol). For the hydrophobic compound Pheida in ethanol  $\tau_T = 0.3$  ms was determined. It should also be noted that the triplet state of Chla is not observable in aqueous solution due to aggregation,<sup>14</sup> whereas it can be detected for the chlorins used here. It can thus be concluded that the hydrophobic ZnPheida component is not completely present in aggregated form, but adopts a monomer–dimer equilibrium as found for Pheida in aqueous solution.<sup>23</sup>

The incorporation of the zinc chlorins into the maquettes extended the triplet lifetime significantly. For the ZnCe6-M1 system in argon- and air-saturated phosphate buffer at pH 7.3,  $\tau_T = 1$  ms and 50  $\mu s$ , respectively. The values for the other three metallopeptides are of comparable magnitude to that of

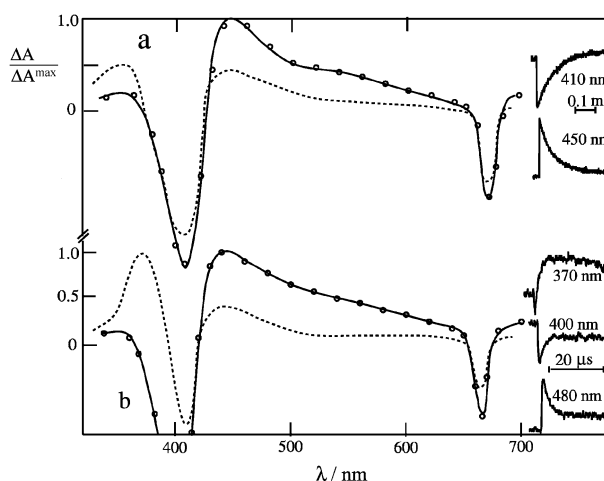


**Fig. 6** Transient absorption spectra of 5  $\mu M$  ZnPheida in argon-saturated 0.01 M phosphate buffer at 24  $^{\circ}C$ , pH 7.3, solid line: at the end of the 420 nm pulse, broken line: after 0.1 ms; in the presence of (a) BQ (10  $\mu M$ , no complex formation) and (b)  $MV^{2+}$  (10  $\mu M$ ); insets: kinetic traces at (a) 410 and 450 nm and (b) 370, 400, and 480 nm as indicated.

**Table 2** Triplet properties of chlorins<sup>a</sup>

Compound	Solvent <sup>b</sup>	$\tau_T$ /ms	$\Phi_{ISC}$ <sup>c</sup>	$k_{ox}/M^{-1} s^{-1} \times 10^9$	$k_q^d/M^{-1} s^{-1} \times 10^9$
<i>Ce6</i>	H <sub>2</sub> O/MeCN	0.05	0.5	0.10	3
	H <sub>2</sub> O/buffer	0.10			
	EtOH	<0.03			
Zn <i>Ce6</i>	H <sub>2</sub> O/buffer	0.40	0.3	0.10	3 (3) <sup>e</sup>
	H <sub>2</sub> O/glycerol	0.10 5.0 <sup>f</sup>			
Zn <i>Ce6</i> -M2	H <sub>2</sub> O/buffer	1.50 [1.0] <sup>h</sup>	0.2	0.03	0.7 [0.8] <sup>h</sup>
ZnPheida	H <sub>2</sub> O/buffer	0.08	<0.1	0.10	3 (3) <sup>e</sup> 2 <sup>g</sup>
	EtOH	0.03		1.50	
ZnPheida-M2	H <sub>2</sub> O/buffer	0.80 [0.5] <sup>h</sup>	<0.1	0.03	0.7

<sup>a</sup> In argon-saturated solution at 24 °C (except for  $k_{ox}$  and  $-50$  °C) and 0.01 M phosphate buffer, pH 7.3 (Zn*Ce6*, pH 10),  $\lambda_{exc} = 420$  nm. <sup>b</sup> H<sub>2</sub>O/MeCN (1 : 1, v/v) and H<sub>2</sub>O/glycerol (2 : 3, v/v). <sup>c</sup> Reference of  $\Phi_{ISC} = 0.5$  for Chl*a* in ethanol.<sup>17</sup> <sup>d</sup> For BQ. <sup>e</sup> Values refer to pHBQ. <sup>f</sup> At  $-50$  °C. <sup>g</sup> Value refers to MV<sup>2+</sup>. <sup>h</sup> Values refer to M1.

the Zn*Ce6*-M1 complex (Table 2 and Fig. 7a and 8a). The T–T absorption at 480 nm ( $\Delta A_{rel}$ ) under optically matched conditions was taken as a measure of the  $\Phi_{ISC}$  value, which is essentially the same for *Ce6* in water or ethanol and for Zn*Ce6* and Zn*Ce6*-M1/-M2 systems in water, but much smaller for ZnPheida and ZnPheida-M1/-M2 complexes in water (Table 2). This result is consistent with the observed low quantum yield of fluorescence for ZnPheida and indicates a high degree of aggregation. The absorbance of the triplet state of ZnPheida in solution and of the peptide-bound ZnPheida systems is much lower than those of Zn*Ce6* and Zn*Ce6*-M1/-M2.

### 3.4 Radical ions

The rate constant of the triplet decay in either air- or argon-saturated aqueous solution shows a linear dependence on the BQ concentration. The slope of the plot of  $1/\tau_T$  vs. [BQ], *i.e.*, the rate constant of quenching by electron transfer, is  $k_q = 3 \times 10^9 M^{-1} s^{-1}$  for Zn*Ce6* and ZnPheida. Examples are shown in Fig. 9. Lower values of  $k_q = (0.7\text{--}0.8) \times 10^9 M^{-1} s^{-1}$  were found for the four zinc chlorin maquettes (Table 2). The triplet yield of the zinc chlorin maquettes remains unchanged upon addition of a forty-fold excess of BQ, whereas the

lifetime (initial decay component) becomes shorter. The triplet lifetime for Zn*Ce6* and ZnPheida, each bound to the peptide M2, is shortened from 1 ms to 50  $\mu$ s upon addition of BQ (Fig. 7 and 8).

The transient observed after triplet decay (Fig. 5b) is due to the radical cation  $C^{\bullet+}$  with maximum at 400 nm, whereas the radical anion  $Q^{\bullet-}$  is virtually not detected due to its low absorption coefficient.<sup>42–44</sup> In order to search for a spectral contribution of the corresponding radical cation, MV<sup>2+</sup>, having a higher molar absorption coefficient in its MV<sup>•+</sup> form at 380 and 420 nm than that of  $Q^{\bullet-}$  at 430 nm,<sup>32,45</sup> was used as alternative electron acceptor. The stronger absorption of the radical MV<sup>•+</sup> with maxima at 380 and 420 nm after 100  $\mu$ s is evident in Fig. 6b.

Temperature dependent measurements in a mixture of aqueous buffer and glycerol (2 : 3, v/v) show that  $1/\tau_T$  of Zn*Ce6* and ZnPheida decrease at lower temperatures due to less efficient self-quenching caused by an increase in solvent viscosity. On the other hand,  $1/\tau_T$  increases upon addition of BQ at a given temperature. Generally,  $k_q$  (*i.e.*, the slope of  $1/\tau_T$  vs. [BQ]) decreases with increasing  $1/T$  (not shown). The radical yield also decreases when the temperature is lowered. At

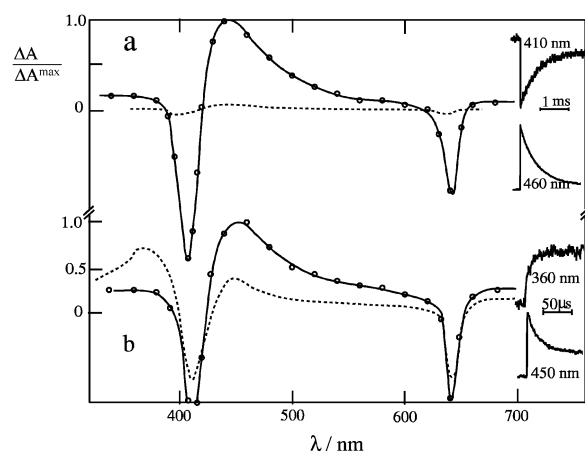


**Fig. 7** Transient absorption spectra of Zn*Ce6*-M2 (6  $\mu$ M) in argon-saturated 0.01 M phosphate buffer at 24 °C, pH 7.3, (a), (b) solid line: at the end of the 420 nm pulse; (a) no additive (broken line: after 1 ms) and (b) in the presence of BQ (10  $\mu$ M, broken line: after 0.1 ms); insets: kinetic traces at (a) 410 and 460 nm and (b) 360 and 450 nm as indicated.

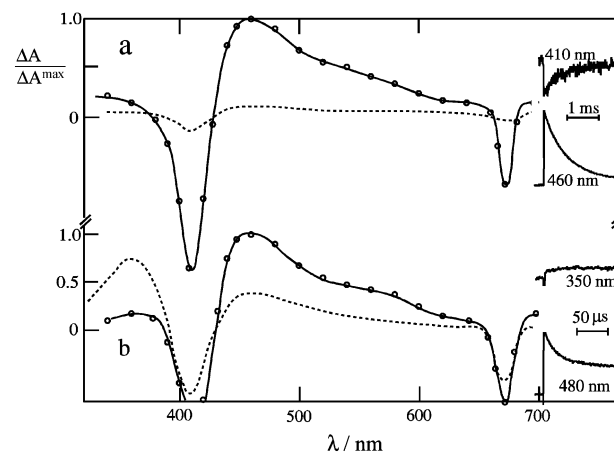


**Fig. 8** Transient absorption spectra of ZnPheida-M2 (6  $\mu$ M) in argon-saturated 0.01 M phosphate buffer at 24 °C, pH 7.3, (a), (b) solid line: at the end of the 420 nm pulse; (a) no additive (broken line: at 1 ms) and (b) in the presence of BQ (10  $\mu$ M, broken line: at 0.1 ms); insets: kinetic traces at (a) 410 and 460 nm and (b) 350 and 480 nm as indicated.

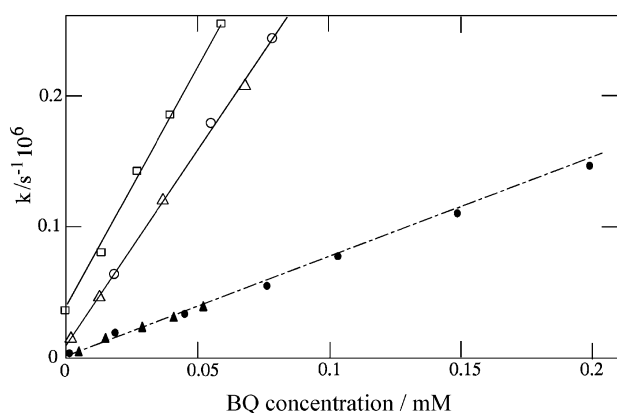


**Fig. 9** Plots of  $1/\tau_T$  vs. [BQ] for ZnCe6/BQ (○), ZnPheida/BQ (△), ZnCe6-M2/BQ (●) and ZnPheida-M2/BQ (▲) in aqueous solution, pH 7.3 and for Chla/BQ in EtOH at 24 °C (□).

–50 °C, for example, the triplet lifetime is *ca.* 5 ms for ZnCe6 and electron transfer was no longer observable. The observed decrease in rate constant of the quenching process at lower temperatures can be explained by an activated process. As the viscosity changes by several orders of magnitude in a small temperature range of *e.g.*, –30 to –60 °C, this is essentially a viscosity-induced activation barrier.

## 4 Discussion

### 4.1 Aggregation behaviour

The observed formation of a new red-shifted band in either the ground state absorption or fluorescence spectra of zinc chlorins in the presence of BQ (Fig. 2 and 3) is reminiscent to changes in the aggregation–disaggregation behaviour. From studies of chlorophyll derivatives in aqueous solution (without quinone addition) the following aggregation pattern has been proposed: a water molecule coordinates *via* its oxygen atom to the  $Mg^{2+}$  atom of one chlorophyll macrocycle and forms a hydrogen bond with the keto C=O function of another chlorophyll molecule:  $Mg \cdots O(H)H \cdots O=C$ .<sup>6</sup> This complexation can also occur with zinc as central metal. For chlorosomal chlorophylls and their more stable zinc analogues, a self-aggregation was found to be driven by intermolecular interaction among the 3<sup>1</sup>-hydroxyl, the central metal and the 13-keto-group.<sup>2–6</sup> High concentrations, low temperatures and dilution by nonpolar solvents shift this equilibrium toward larger self-assembled species. For Ce6 it was also found that a decrease of the pH to 2.7 leads to an increase in hydrophobicity, which is related to the protonation of the compound.<sup>24</sup> The variability of the tendency to aggregate, which is visible through a red-shift of the absorption bands, is therefore related to changes in the chemical structure. However, none of these descriptions apply to the present systems, because neither a 3<sup>1</sup>-hydroxyl group is present in the chemical structure of the chlorins, nor were measurements carried out below pH 7.3.

We propose (see also ref. 20 and 23) that aggregation does not take place for Ce6, whereas for Pheida in aqueous solution a monomer–dimer equilibrium describes the situation. For

Pheida in methanol/heavy water (1 : 20, v/v) solution (heavy water in that case being applied for better singlet oxygen detection) a quantum yield of singlet oxygen production of  $\Phi_{\Delta} \leq 0.02$  was found,<sup>16</sup> *i.e.*, aggregation suppresses intersystem crossing. The yield, however, increases to  $\Phi_{\Delta} = 0.7$ , when Triton X-100 is added, favouring the monomeric form of Pheida with high  $\Phi_{ISC}$ .<sup>16</sup> Similar to Pheida the fraction of monomeric Chla decreases upon addition of water and a triplet of Chla aggregates was not detected.<sup>14</sup> Besides an addition of a surfactant, the aggregation of Chla in aqueous solution can also be suppressed by addition of *de novo* peptides.<sup>19</sup> In contrast, we did not find an increase of  $\Phi_I$  and  $\Phi_{ISC}$  for ZnPheida upon incorporation into the maquettes (Tables 1 and 2). Currently, this observation cannot be explained satisfactorily. However, we can exclude aggregation as a cause for these low values, since the spectral properties (bathochromic shifts in absorbance and fluorescence) indicate that the pigments are monomeric and bound within the maquettes, and no excess of free chlorin is present.

### 4.2 Complex formation between zinc chlorins and BQs

The ground state absorptions of metal-free chlorins and the fluorescence excitation spectra above *ca.* 400 nm are similar in the presence and absence of BQs. In contrast, ZnCe6 and ZnPheida show a bathochromic shift upon BQ addition (Table 1), which is not observed for maquette incorporated zinc chlorins. A specific interaction between the zinc-containing pigment and a quinone should therefore be considered. These findings may be compared to examples from the literature where porphyrins containing appropriate hydroxyphenol substituents and BQs show specific interactions.<sup>29–31</sup> These ubiquinone analogues and functional porphyrins interact *via* multiple hydrogen bonds, but no metal ion is required, in contrast to the chlorin cases presented here.

The novel stable band is proposed to be due to complex formation between BQ and ZnCe6. It is suggested to be formed in two steps, as indicated by the dependence of the rate constant  $k_-$  for the decay of the Soret and  $Q_y$  absorption bands on the BQ concentration, and the rate constant  $k_+$  for the increase of the new band (Fig. 2 and 3). The new generated absorption bands of ZnPheida at 738 nm induced by BQ and at 685 nm mediated by imidazole, give evidence for two different types of complexes. Although the structure of the complex is not known, a quinone-assisted conversion of the chlorin monomer into an aggregate and a water-assisted conversion into another aggregate are considered to be in accordance with the two-step kinetics (Fig. 4) and the pronounced red-shifts in absorption<sup>13</sup> and fluorescence (Fig. 3 and Table 1).

### 4.3 Electron transfer from the chlorin triplet state to BQ

Dynamic quenching by BQs in polar solvents has been studied for Chla.<sup>9–12</sup> For the presented chlorin–quinone systems, reactions (1)–(4) in Scheme 1 show reversible photooxidation *via* the excited singlet state, ISC, electron transfer and charge recombination of the two ions,  $C^{\bullet+}$  and  $Q^{\bullet-}$ .<sup>7–12</sup> All other decay processes of  $^3C^*$  in the given system, even quenching by traces of oxygen, play no significant role due to the dominance

of reaction (2). The radicals, *i.e.*, pigment cation and quinone anion, have already been characterized by different groups.<sup>42–44</sup> At pH > 4 in aqueous solution (as in our experiments) the equilibrium between Q<sup>•-</sup> and the conjugated acid (semiquinone radical HQ<sup>•</sup>) lies on the anion side.<sup>45</sup> The radical pair, <sup>3</sup>(C<sup>•+</sup> Q<sup>•-</sup>), which is the direct result of the quenching process, can separate into the chlorin cation radical, C<sup>•+</sup>, and the quinone anion radical, reaction (3). In principle, a reaction of the separated Q<sup>•-</sup> and C<sup>•+</sup> to different products is possible, reaction (5).<sup>8</sup> Product formation is in competition with charge recombination, reaction (4), but its occurrence is unlikely at ambient temperature. A typical rate constant for back electron transfer is  $k_4 = 2 \times 10^9 \text{ M}^{-1} \text{ s}^{-1}$ .<sup>8–11</sup>

The transient absorption spectra of <sup>3</sup>C\* and C<sup>•+</sup> are overlapping and partly similar. For <sup>3</sup>Chla\* and Chla<sup>•+</sup> the molar absorption coefficients are  $\epsilon_{460} = 3.5 \times 10^4$  and  $\epsilon_{400} = 3.5 \times 10^4 \text{ M}^{-1} \text{ cm}^{-1}$ , respectively.<sup>42–44</sup> For chlorins in aqueous solution the T–T absorption and radical cation properties are not documented, thus values of  $\epsilon_{\text{max}} = 4 \times 10^4 \text{ M}^{-1} \text{ cm}^{-1}$  were taken for <sup>3</sup>C\* and C<sup>•+</sup>. The spectra of the semiquinone radical, HQ<sup>•</sup> and the radical anion, Q<sup>•-</sup> are only slightly shifted in aqueous solution. They are characterized by two peaks around 320 and 430 nm with molar absorption coefficient for parent BQ:  $\epsilon_{420} = 0.6 \times 10^4 \text{ M}^{-1} \text{ cm}^{-1}$ .<sup>45</sup> Hence, in comparison with the absorption coefficients of <sup>3</sup>C\* and C<sup>•+</sup> the transient absorption of Q<sup>•-</sup> is masked by that of C<sup>•+</sup> and therefore not detectable in our transient spectra.

Addition of up to a forty fold excess of quinone to the zinc chlorins does not influence the fluorescence lifetime. Thus <sup>1</sup>C\* of zinc chlorins does not participate in the electron transfer as already concluded for a related case.<sup>12</sup> This is in contrast to native photosystems, where the electron transfer occurs from the singlet excited state.

A significant effect on photoinduced electron transfer from ZnCe6 in aqueous solution to phBQ was already observed by EPR for a peptide with a sequence similar to M2.<sup>36</sup> Under our conditions, the yield of the radical cation formation is essentially unchanged (see section 3.4), but the efficiency, as expressed by  $k_q = 3 \times 10^9 \text{ M}^{-1} \text{ s}^{-1}$  for the zinc chlorins in aqueous solution *vs.*  $k_q = 7 \times 10^8$  and  $8 \times 10^8 \text{ M}^{-1} \text{ s}^{-1}$  for the zinc chlorins bound to the peptides M2 and M1 (Table 2), is about four times reduced. The smaller electron transfer rate is due to shielding of the zinc chlorin by the four-helix bundle. Nevertheless, the observed quenching rate constants are in quite good agreement with the literature values for pigment quenching by BQ.<sup>9–12</sup> The triplet state of zinc protoporphyrin IX in a synthetic four-helix bundle protein in aqueous solution is also quenched by AQS with  $k_q = 0.5 \times 10^9 \text{ M}^{-1} \text{ s}^{-1}$ .<sup>35b</sup> The  $k_q$  values for triplet quenching by BQ of the chlorins (Table 2), Chla and zinc tetraphenylporphyrin are close to the diffusion-controlled limit.<sup>26,28</sup> Significant differences with respect to ligation, absorption and fluorescence behaviour between the peptides M1 and M2 were not observed.

## 5 Conclusion

Light-induced electron transfer processes from zinc chlorins (ZnCe6 and ZnPheida) in aqueous solution as well as incor-

porated in peptides to noncovalently bound quinones were investigated. The aim was to study the influence of peptides on the electron transfer process from excited free and bound zinc chlorins to quinones. ZnCe6 and ZnPheida show a steady-state interaction with quinones which is evident by a new absorption band at longer wavelengths. In contrast, this complex formation induced by the quinone was not found for the metal free compounds (Ce6 and Pheida) and is also absent for the four different metallopeptides (ZnPheida-M1, ZnPheida-M2, ZnCe6-M1, ZnCe6-M2).

ZnCe6 in solution as well as bound to the peptides shows substantial quantum yields of fluorescence and intersystem crossing, whereas both values are lower for the ZnPheida systems. This suggests that ZnCe6 shows no aggregation, but ZnPheida has a higher tendency to aggregate. Nevertheless, both pigments could be studied by fluorescence and transient absorption spectroscopy, which is not feasible for Chla in aqueous solution.

The triplet state is quenched by BQs *via* electron transfer and the observed radical cations of the zinc chlorins essentially decay by “reverse” electron transfer from the quinone radical anion. In comparison to unbound zinc chlorins, the pigment–peptide complexes as a model system for a reaction center show much longer triplet lifetimes and four times lower rate constants of quenching by quinones, indicating shielding of the pigments by the peptides.

This work describes some of the difficulties and the notable complexity on the way to synthesize an artificial reaction center. The necessary conditions are that the pigments are ligated by the peptides to prevent complex formation with the acceptor molecule, but the peptides have to be as small as possible in order to keep the distance between the donor and acceptor molecule small enough to allow efficient electron transfer. As a major finding we demonstrate that in model systems, similar to nature, a covalent attachment of a quinone to the peptide is not essential.

## Acknowledgements

We thank the Deutsche Forschungsgemeinschaft (SFB 663, subproject A7) for financial support, M. van Gestel for helpful discussions, and I. Heise, M. Trinoga, G. Koc-Weier, N. Dickmann and L. J. Currell for technical assistance.

## References

- 1 R. E. Blankenship, in *Molecular Mechanisms of Photosynthesis*, Blackwell Science, Oxford, 2002.
- 2 (a) J. Chiefari, K. Griebenow, N. Griebenow, T. S. Balaban, A. R. Holzwarth and K. Schaffner, *J. Phys. Chem.*, 1995, **99**, 1357; (b) T. S. Balaban, A. R. Holzwarth, K. Schaffner, G.-J. Boender and H. J. M. de Groot, *Biochemistry*, 1995, **34**, 15259; (c) T. Mizoguchi, S. Sakamoto, Y. Koyama, K. Ogura and F. Inagaki, *Photochem. Photobiol.*, 1998, **67**, 239.
- 3 H. Tamiaki, M. Amakawa, A. R. Holzwarth and K. Schaffner, *Photosynth. Res.*, 2002, **71**, 59.
- 4 H. Tamiaki, *Photochem. Photobiol. Sci.*, 2005, **4**, 675.
- 5 T. Miyatake, H. Tamiaki, M. Fujiwara and T. Matsushita, *Bioorg. Med. Chem.*, 2004, **12**, 2173.
- 6 T. S. Balaban, H. Tamiaki and A. R. Holzwarth, *Top. Curr. Chem.*, 2005, **258**, 1.
- 7 C. Bohne, A. Faljoni-Arário and G. Cilento, *Photochem. Photobiol.*, 1988, **48**, 341.

- 8 A. K. Chibisov, *Photochem. Photobiol.*, 1969, **10**, 331.
- 9 J. Kelly and G. Porter, *Proc. R. Soc. London, Ser. A*, 1970, **319**, 319.
- 10 B. J. Hales and J. R. Bolton, *J. Am. Chem. Soc.*, 1972, **94**, 3314.
- 11 (a) P. G. Bowers and G. Porter, *Proc. R. Soc. London, Ser. A*, 1967, **296**, 435; (b) R. G. Brown, A. Harriman and L. Harris, *J. Chem. Soc., Faraday Trans. 2*, 1978, 1193; (c) F. Castelli, G. Cheddar, F. Rizzuto and G. Tollin, *Photochem. Photobiol.*, 1979, **29**, 153; (d) R. H. Clarke, D. R. Hobart and W. R. Leenstra, *J. Am. Chem. Soc.*, 1979, **101**, 2416.
- 12 F. Castelli, in *Laser Application in Chemistry*, ed. K. L. Kompa and J. Wanner, NATO Series B, Plenum Press, New York, 1984, vol. 105, pp. 225.
- 13 (a) K. Uehara, Y. Hioki and M. Mimuro, *Photochem. Photobiol.*, 1993, **58**, 127; (b) R. Vladkova, *Photochem. Photobiol.*, 2000, **71**, 71.
- 14 A. K. Chibisov, T. D. Slavnova and H. Görner, *J. Photochem. Photobiol., B*, 2003, **72**, 11.
- 15 (a) H. Scheer and J. J. Katz, *J. Am. Chem. Soc.*, 1978, **100**, 561; (b) J. J. Katz, *Spectrum*, 1994, **7**, 1; (c) G. W. Kenner, S. W. McCombie and K. M. Smith, *J. Chem. Soc., Perkin Trans. 2*, 1973, 2517; (d) H. Scheer, R. J. Porra and J. M. Anderson, *Photochem. Photobiol.*, 1989, **50**, 403; (e) T. Suzuki and Y. Shioi, *Photosynth. Res.*, 2002, **74**, 217.
- 16 C. Tanielian, C. Wolff and M. Esch, *J. Phys. Chem.*, 1996, **100**, 6555.
- 17 M. Jabben, N. A. Garcia, S. E. Braslavsky and K. Schaffner, *Photochem. Photobiol.*, 1986, **43**, 127.
- 18 A. Agostiano, L. Catucci, G. Colafemmina and H. Scheer, *J. Phys. Chem. B*, 2002, **106**, 1446.
- 19 A. Dudkowiak, C. Nakamura, T. Arai and J. Miyake, *J. Photochem. Photobiol., B*, 1998, **45**, 43.
- 20 B. Roeder and H. Wabnitz, *J. Photochem. Photobiol., B*, 1987, **1**, 103.
- 21 J. D. Spikes and J. C. Bommer, *J. Photochem. Photobiol., B*, 1993, **17**, 135.
- 22 S. V. Kuznetsov, M. Bazin and R. Santus, *J. Photochem. Photobiol., A*, 1997, **103**, 57.
- 23 I. Eichwurzel, H. Stiel and B. Roeder, *J. Photochem. Photobiol., B*, 2000, **54**, 194.
- 24 B. Čunderlíková, L. Gangeskar and J. Moan, *J. Photochem. Photobiol., B*, 1999, **53**, 81.
- 25 C. Brückner, J. R. McCarthy, H. W. Daniell, Z. D. Pendon, R. P. Ilagan, T. M. Francis, L. Ren, R. R. Birge and H. A. Frank, *Chem. Phys.*, 2003, **294**, 285.
- 26 M. Ebersole, P. R. Levstein and H. van Willigen, *J. Phys. Chem.*, 1992, **96**, 9310.
- 27 (a) G. Porter, *Proc. R. Soc. London, Ser. A*, 1978, **362**, 281; (b) W. E. Ford and G. Tollin, *Photochem. Photobiol.*, 1983, **38**, 441; (c) P. R. Levstein and H. van Willigen, *Chem. Phys. Lett.*, 1991, **187**, 415; (d) S. Fukuzumi, K. Ohkubo, H. Imahori, J. Shao, Z. Ou, G. Zheng, Y. Chen, R. K. Pandey, M. Fujitsuka, O. Ito and K. M. Kadish, *J. Am. Chem. Soc.*, 2001, **123**, 10676; (e) P. P. Mishra, J. Bhatnagar and A. Datta, *Chem. Phys. Lett.*, 2004, **386**, 158; (f) T. K. Mukherjee, P. P. Mishra and A. Datta, *Chem. Phys. Lett.*, 2005, **407**, 119.
- 28 G. J. Kavarnos and N. J. Turro, *Chem. Rev.*, 1986, **86**, 401.
- 29 (a) T. Buranda, N. Soice, S. Lin, R. Larsen and M. Ondrias, *J. Phys. Chem.*, 1996, **100**, 18868; (b) T. Buranda, M. Enlow, J. Griener, N. Soice and M. Ondrias, *J. Phys. Chem. B*, 1998, **102**, 9081.
- 30 K. Okamoto, K. Ohkubo, K. M. Kadish and S. Fukuzumi, *J. Phys. Chem. A*, 2004, **108**, 10405.
- 31 (a) Y. Aoyama, M. Asakawa, Y. Matsui and H. Ogoshi, *J. Am. Chem. Soc.*, 1991, **113**, 6233; (b) T. Hayashi, T. Miyahara, N. Koide, Y. Kato, H. Masuda and H. Ogoshi, *J. Am. Chem. Soc.*, 1997, **119**, 7281; (c) H. Ogoshi and T. Mizutani, *Curr. Opin. Chem. Biol.*, 1999, **3**, 736; (d) F. D'Souza and G. R. Deviprasad, *J. Org. Chem.*, 2001, **66**, 4601; (e) A. Tsuda, C. Fukumoto and T. Oshima, *J. Am. Chem. Soc.*, 2003, **125**, 5811; (f) J. R. Darwent, P. Douglas, A. Harriman, G. Porter and M. C. Richoux, *Coord. Chem. Rev.*, 1982, **44**, 83.
- 32 T. Watanabe and K. Honda, *J. Phys. Chem.*, 1982, **86**, 2617.
- 33 H. A. Montejano, M. Gervaldo and S. G. Bertolotti, *Dyes Pigm.*, 2005, **64**, 117.
- 34 N. De Jonge, H. K. Rau and W. Haehnel, *Z. Phys. Chem.*, 1999, **213**, 175.
- 35 (a) M. Fahnenschmidt, R. Bittl, E. Schlodder, W. Haehnel and W. Lubitz, *Phys. Chem. Chem. Phys.*, 2001, **3**, 4082; (b) M. Fahnenschmidt, R. Bittl, H. K. Rau, W. Haehnel and W. Lubitz, *Chem. Phys. Lett.*, 2000, **323**, 329.
- 36 M. R. Razeghifard and T. Wydrzynski, *Biochemistry*, 2003, **42**, 1024.
- 37 S. Hay, B. B. Wallace, T. A. Smith, K. P. Ghiggino and T. Wydrzynski, *Proc. Natl. Acad. Sci. U. S. A.*, 2004, **101**, 17675.
- 38 D. E. Robertson, R. S. Farid, C. C. Moser, J. L. Urbauer, S. E. Mulholland, R. Pidikiti, J. D. Lear, A. J. Wand, W. F. DeGrado and P. L. Dutton, *Nature*, 1994, **368**, 425.
- 39 R. E. Sharp, J. R. Diers, D. F. Bocian and P. L. Dutton, *J. Am. Chem. Soc.*, 1998, **120**, 7103.
- 40 A. Mennenga, PhD Thesis, Heinrich-Heine-Universität, Düsseldorf, 2007.
- 41 W. R. Scheidt and D. M. Chipman, *J. Am. Chem. Soc.*, 1986, **108**, 1163.
- 42 (a) T. Watanabe and K. Honda, *J. Am. Chem. Soc.*, 1980, **102**, 370; (b) J. Kiwi and M. Grätzel, *J. Phys. Chem.*, 1980, **84**, 1503.
- 43 J.-P. Chauvet, R. Viovy, R. Santus and E. J. Land, *J. Phys. Chem.*, 1981, **85**, 3449.
- 44 H. Levanon and P. Neta, *J. Phys. Chem.*, 1982, **86**, 4532.
- 45 (a) V. A. Roginsky, L. M. Pisarenko, W. Bors, C. Michel and M. Saran, *J. Chem. Soc., Faraday Trans.*, 1998, **94**, 1835; (b) S. Steenken and P. Neta, in *The Chemistry of Phenols*, ed. Z. Rappoport, Wiley, New York, 2003, p. 1107.